Bulletin of Electrical Engineering and Informatics
Vol. 14, No. 6, December 2025, pp. 4316~4324
ISSN: 2302-9285, DOI: 10.11591/eei.v14i6.9653

Application of traction force observer and sliding mode controller for speed in enhancing the stability of electric vehicles

An Thi Hoai Thu Anh, Nguyen Van Hoa
Department of Electrical Engineering, Faculty of Electrical-Electronic Engineering, University of Transport and Communications, Hanoi, Vietnam

Article Info

Article history:

Received Dec 5, 2024
Revised Oct 3, 2025
Accepted Oct 14, 2025

Keywords:

Carsim
Electric vehicles
Sliding mode control
Traction force distribution
Traction force observation

ABSTRACT

With the rapid advancement of electric vehicle (EV) technology, optimizing control and stability has become a key research focus. One major challenge is efficiently distributing traction force while minimizing disturbances under real-world conditions. This paper proposes a traction force observation method combined with a sliding mode speed controller to enhance EV performance. The observation method estimates the traction force from the motor to the wheels and detects disturbances affecting force transmission. This enables optimal traction force distribution among the wheels, reducing slip, improving road grip, and enhancing stability in complex driving conditions. Meanwhile, the sliding mode controller flexibly adjusts traction force as the vehicle navigates various terrains, ensuring stability and safety in hazardous situations. Simulations conducted using MATLAB Simulink and CarSim demonstrate that the proposed system significantly improves EV stability and control performance. Although these results are promising, further studies are necessary to address real-world implementation challenges and optimize the method for practical applications, including parameter tuning, sensor integration, and experimental validation. Overall, this research provides a practical framework for enhancing traction control and vehicle dynamics in future intelligent electric mobility systems.

Corresponding Author:

An Thi Hoai Thu Anh
Department of Electrical Engineering, Faculty of Electrical-Electronic Engineering
University of Transport and Communications
No. 3 Cau Giay, Lang Commune, Hanoi, Vietnam
Email: htanh.ktd@utc.edu.vn

1. INTRODUCTION

Electric vehicles (EVs) are gradually becoming a global trend due to their advantages in energy efficiency, environmental protection, and reduced dependence on fossil fuels [1], [2]. However, ensuring the stability and control capabilities of EVs under various operating conditions remains a significant challenge for researchers and engineers. In real-world operating environments, the speed and traction of EVs are often influenced by road conditions, load, and weather [3], [4]. These fluctuations impact operational efficiency and compromise the vehicle's stability, thereby increasing the risk of loss of control and safety hazards while driving [5], [6]. Therefore, developing advanced control systems to improve speed and traction control is urgently needed.

Speed and traction control are two critical factors in ensuring the performance and stability of EVs. However, speed control often faces challenges when the car moves on road surfaces with varying friction or when the load changes rapidly [7], [8]. The uneven traction between the wheels and the road can cause wheel slip and instability, reducing the vehicle's ability to be controlled accurately [9], [10]. In traditional systems,

traction control mainly relies on feedback from sensors. Still, these sensors are often affected by delays and errors, leading to an inability to respond promptly to rapid fluctuations [11]-[13]. This increases the risk of instability when the vehicle is moving at high speeds or under poor road conditions.

Colli *et al*. [14] proposed a longitudinal control method based on a configuration that utilises a grip estimation model and a slip controller. These two controllers could track the grip value without requiring knowledge of the road conditions. Jin and Liu [15] established an adaptive sliding mode controller to enhance stability in EV scenarios, while also proposing a method for estimating the lateral slip angle. A supervisory controller for vehicle operation in cases of blockages or turns was suggested by Ringdorfer and Horn [16]. Jin *et al*. [17], presents an optimised longitudinal slip ratio system for real-time identification of EVs with in-wheel motors, proposed based on the adhesion between the tyre and the road surface. The controller ensures anti-lock and anti-slip functions by distributing interventions between braking and motor control for the wheel drive. Jia *et al*. [18] designed a new piecewise linear (PWL) traction controller for EVs with in-wheel motors. The traction controller decomposes the traction moment into a straight transmission control moment to monitor the slip ratio.

This study proposes the application of a traction force observer combined with a sliding mode controller for speed control in the traction control system of EVs. The traction force observer helps to monitor and accurately estimate the traction force between the wheels and the road, providing input information for the traction force distribution module. Based on data from the traction force distribution module, the sliding mode controller for speed will precisely adjust each wheel's speed, ensuring optimal control even when road conditions change abruptly. Combining the traction force observer and the sliding mode controller for speed helps maintain vehicle stability and improves acceleration performance, optimising torque distribution between the wheels. This enhances the vehicle's operational efficiency in all environmental conditions, while reducing the risk of wheel slip and loss of control. Finally, simulation results will demonstrate the correctness and effectiveness of the proposed methods.

2. MODELING OF ELECTRIC VEHICLES

The first step in the research process is to develop the algorithm and model the system. For a motor integrated into all four wheels, as in this study, the vehicle model has the structure shown in Figure 1, including the traction motor model, dynamic model, kinematic model, and position model.

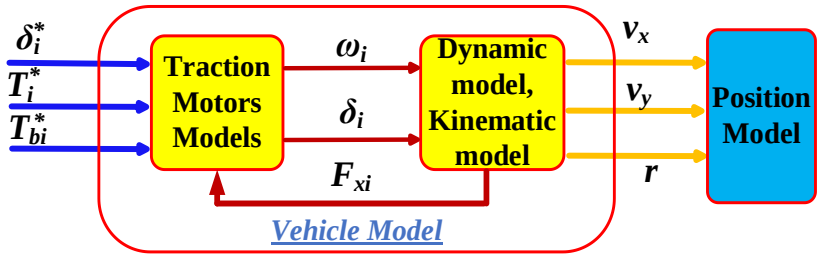

Figure 1. Structure of the independent four-wheel drive vehicle model

Where δ_i^*, T_i^*, T_{bi}^* being the steering angle, applied torque, and braking torque, respectively, r, v_x, and vy representing the angular velocity, longitudinal velocity, and lateral velocity at the centre of gravity (COG).

2.1. Powertrain model of electric vehicle

The powertrain is the link between the energy source and the wheels, ensuring the smooth operation of the EV. This system distributes torque to each wheel, generating the necessary traction for moving the car [19]. To describe this process in detail, the mathematical model for each wheel is as (1):

$$T_d = \frac{K_m}{\tau_m s+1} T_d^* \quad (1)$$

Where K_m is the motor gain factor, τ_m is the time constant, and T_d is the driving torque.
We have the following torque equilibrium equation for each wheel:

$$T_d - R_{eff} F_x - k_b T_b = J_x \frac{d\omega}{dt} \quad (2)$$

Where J_x is the moment of wheel inertia and k_bT_b represents the braking torque.

2.2. Kinematic model of electric vehicle

Assuming that the vehicle's COG remains constant throughout the motion, we can place the coordinate system at the vehicle's COG. This simplifies the calculations in the vehicle's kinematic and dynamic model. According to [20], [21], the equation represents the relationship between the vehicle's kinematics and dynamics as (3):

$$M\dot{v} + C(v) = \tau \tag{3}$$

Where m is the inertia matrix, $C(v)$ is the Coriolis matrix and τ_z vector representing the torque, τ is the moment of rotation around the vertical axis passing through the vehicle's COG.

From in (3), the equilibrium equation represents the relationship between the applied forces, acceleration, and velocity as (4):

$$\begin{cases} F_x = m\dot{v}_x - mrv_y \\ F_y = m\dot{v}_y + mrv_x \end{cases} \tag{4}$$

Applying Newton's second law and substituting the forces and accelerations, in (4) can be rewritten as (5):

$$\begin{cases} \dot{v}_x = a_x + rv_y \\ \dot{v}_y = a_y - rv_x \end{cases} \tag{5}$$

2.3. Dynamic model of electric vehicle

According to [22]-[24], the force acting on each wheel is represented as (6):

$$\begin{cases} ma_x = (F_{x1}\cos\delta_1 + F_{x2}\cos\delta_2) - \left(F_{y1}\sin\delta_1 + F_{y2}\sin\delta_2\right) + F_{x3} + F_{x4} - F_{res} \\ ma_x = (F_{x1}\sin\delta_1 + F_{x2}\sin\delta_2) - \left(F_{y1}\cos\delta_1 + F_{y2}\cos\delta_2\right) + F_{y3} + F_{y4} \\ J_z\dot{r} = \left(l_fF_{x1}\sin\delta_1 + l_fF_{x2}\sin\delta_2\right) + \left(l_fF_{y1}\cos\delta_1 + l_fF_{y2}\cos\delta_2\right) - l_f\left(F_{y3} + F_{y4}\right) \\ -\frac{1}{2}b_f(F_{x1}\cos\delta_1 + F_{x2}\cos\delta_2) + \frac{1}{2}b_f\left(F_{y1}\sin\delta_1 - F_{y2}\sin\delta_2\right) - \frac{1}{2}b_r\left(F_{y3} - F_{y4}\right) \end{cases} \tag{6}$$

Where m is the vehicle mass, J_z is the moment around *z-axis*, F_{xi}, F_{yi} forces acting on the wheel in the longitudinal and lateral directions of the wheel axis, a_x, a_y is the longitudinal and transverse acceleration COG, l_f, l_r, b_f, b_r describe the geometric characteristics of the vehicle, F_{res} is the total resistive force, ρ is natural gas thickness, A_F is resistance area, C_d is drag coefficient, c_{rr} is coefficient of rolling friction, and g is the acceleration of gravity.

Ignoring the effect of wind, the total resistive force F_{res} is determined by (7):

$$F_{res} = F_{air} + F_{roll} = C_dA_F\frac{\rho}{2}v_x^2 + c_{rr}mg \tag{8}$$

3. CONTROL DESIGN

Figure 2 shows the control structure for the longitudinal control of an EV during acceleration, specifically, the steering force distribution control. In this context, the traction force observation method and the speed controller using the SMC algorithm are illustrated. Since only the case of straight-line acceleration is considered, the steering angle δ_{dr} and the braking torque T_{br} are set to zero.

3.1. Design of speed controller using sliding mode control algorithm

We have a discrepancy between the desired value and the response $e = \omega - \omega^*$, in which ω^* is the desired value. Substitute in (2) and take the error derivative to get:

$$\dot{e} = \dot{\omega} - \dot{\omega}^* = \frac{T_d}{J_x} - \frac{R_{eff}F_x}{J_x} - \frac{k_bT_b}{J_x} - \dot{\omega}^*$$

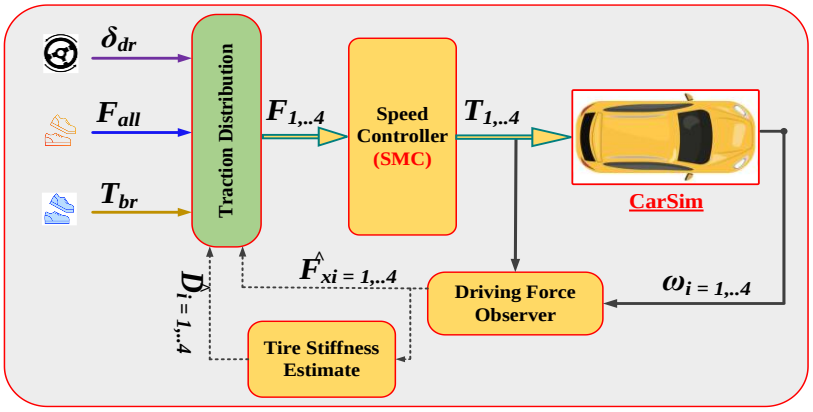

Figure 2. Steering force distribution structure using a traction force observer and SMC controller

Choose the Lyapunov function $V = \frac{1}{2}s^2$. Derivative *V*, obtained:

$$\dot{V} = s.\dot{s} \tag{9}$$

To ensure the stability condition, we have the sliding surface s defined:

$$s = e \Rightarrow \dot{s} = \dot{e}$$

Thus $\dot{s} = 0$, we obtain the stable control component as (10):

$$T_d = J_x\dot{\omega}^* + R_{eff}F_x + k_bT_b \tag{10}$$

One of the above laws can be chosen to ensure the system's quality. In this paper, the exponential reaching law is selected [25]-[27], which has (11):

$$\dot{s} = -\varepsilon\, sgn(s) - ks, \varepsilon > 0, k > 0 \tag{11}$$

Therefore, the SMC control signal is designed in (12):

$$\frac{T_d}{J_x} - \frac{R_{eff}F_x}{J_x} - \frac{k_bT_b}{J_x} - \dot{\omega}^* = -\varepsilon\, sgn(s) - ks \Rightarrow T_d = -J_x\varepsilon\, sgn(s) - J_xks + R_{eff}F_x + J_x\dot{\omega}^* + k_bT_b \tag{12}$$

From (16), SMC for the 4-wheel drive is rewritten as (13):

$$T_i = -J_x\varepsilon\, sgn(s) - k_{\omega_i}e_{\omega i} + R_{eff}F_x + J_x\frac{d\omega}{dt} \tag{13}$$

The derivative of *V* is:

$$T_i = -J_x\varepsilon\, sgn(s) - k_{\omega_i}e_{\omega i} + R_{eff}F_x + J_x\frac{d\omega}{dt} \tag{14}$$

Substituting (16) into (18), the stability shown in (19) demonstrates the method's correctness.

$$\dot{V} = s(-ks - \varepsilon\, sgn(s)) = -(\varepsilon|s| + ks^2) \leq 0 \tag{15}$$

3.2. Designing the traction force observer

To effectively control the driving process, the controller must distribute the steering force properly to minimize wheel slip. Therefore, accurately estimating the steering force is crucial. Based on the mathematical model of the four-wheel drive system during acceleration, (2) can be rewritten as (16):

$$T_d - R_{eff}F_x = J_x\dot{\omega} \Rightarrow \dot{\omega} = \frac{1}{J_x}T_d - \frac{R_{eff}F_x}{J_x} \tag{16}$$

Let $x = \omega$, $g = \frac{1}{J_x}$, $u = T_d$, $d = -\frac{R_{eff} F_x}{J_x}$ be substituted into (20), we obtain:

$$\dot{x} = gu + d \tag{17}$$

Where u is the control variables, d represents the steering force, and the estimation error is defined as (18):

$$\tilde{d} = d - \hat{d} \tag{18}$$

With the disturbance estimation, (21) can be rewritten as (19):

$$\dot{\hat{d}} = \frac{1}{\varepsilon}\left(\dot{x} - gu - \hat{d}\right) \tag{19}$$

We have the observation coefficient $1/\varepsilon$ as a positive constant. The auxiliary state variable ξ is defined as (20):

$$\xi = \hat{d} - \frac{x}{\varepsilon} \tag{20}$$

From the equation, the derivative of the auxiliary state variable ξ is given by (21):

$$\dot{\xi} = -\frac{1}{\varepsilon}\left(\xi + \frac{x}{\varepsilon}\right) - \frac{1}{\varepsilon} gu \tag{21}$$

From (24) and (25), the estimation error can be expressed as (22):

$$\dot{\tilde{d}} = -\frac{1}{\varepsilon}\tilde{d} + \dot{d} \tag{22}$$

4. RESULTS AND DISCUSSION

The simulation results will be conducted using MATLAB/Simulink in conjunction with CarSim, with the EV parameters set in the CarSim software, as shown in Table 1.

Table 1. The vehicle parameters table used in the simulation

Quantity	Notation	Value	Quantity	Notation	Value
Vehicle mass	m	1270 kg	Distance between the two front wheels	B_f	1.675 m
Wheel radius	R_{eff}	0.32 m	Distance between the two rear wheels	B_r	1.675 m
Wheelbase	L	2.91 m	Drag area	A	2.2 m^2
Length from front axle-COG	L_f	1.105 m	Wheel inertia	J_w	2 N.m
Length from rear axle-COG	L_f	1.898 m	Centre height to ground	h	0.54 m

Figure 3 illustrates the road simulation scenarios for the EV. The concrete road represents a high-friction surface with a coefficient of friction of approximately 0.85. In contrast, the snow road corresponds to a low-friction surface with a coefficient of friction of around 0.2.

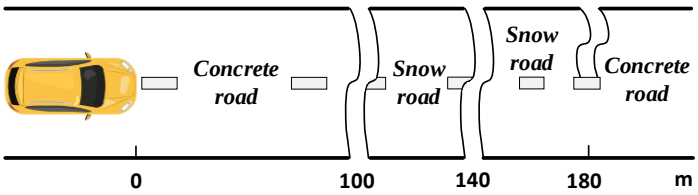

Figure 3. Simulated paragraph on carsim software

Figure 4 illustrates that the vehicle and wheel speeds have increased gradually over time, indicating the acceleration process. Figure 4(a) is the vehicle's linear speed, and Figure 4(b) is the wheel speed. When

entering slippery road conditions, the speed fluctuates only slightly and insignificantly, indicating that the system operates stably and is not affected by varying road conditions.

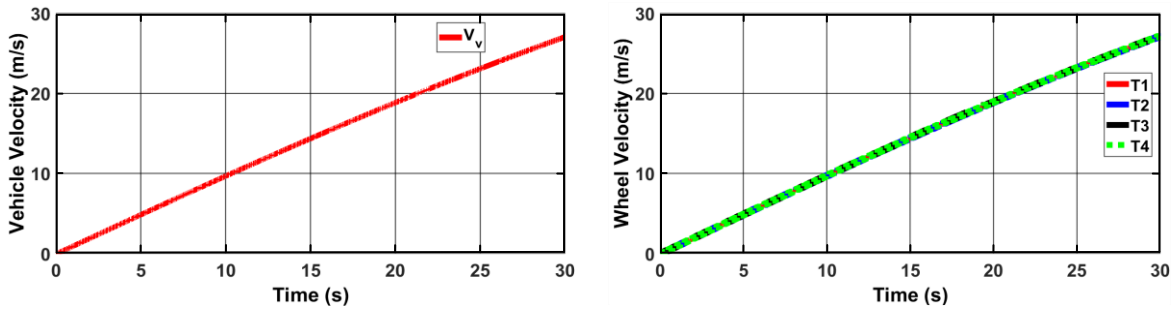

Figure 4. Vehicle speed and wheel speed: (a) and (b) wheel speed

The traction force, torque, and slip responses are illustrated in Figure 5. With a total applied force of 1500 N in Figure 5(a), the distributed forces closely follow the total applied force, demonstrating that the force distribution among the wheels is well-balanced. The traction force and torque shown in Figures 5(b) and (c) exhibit changes consistent with the road conditions set. When zoomed in on Figure 5(c), it can be observed that the torque of the left wheels decreases while the torque of the right wheels increases as the vehicle encounters slippery road conditions. Upon returning to a high-friction road surface, the traction forces and torques of the left and right wheels change inversely to maintain the total traction force in alignment with the set value. The slip ratio in Figure 5(d) is approximately zero, indicating that the vehicle operates stably without wheel slippage when driving on snowy roads.

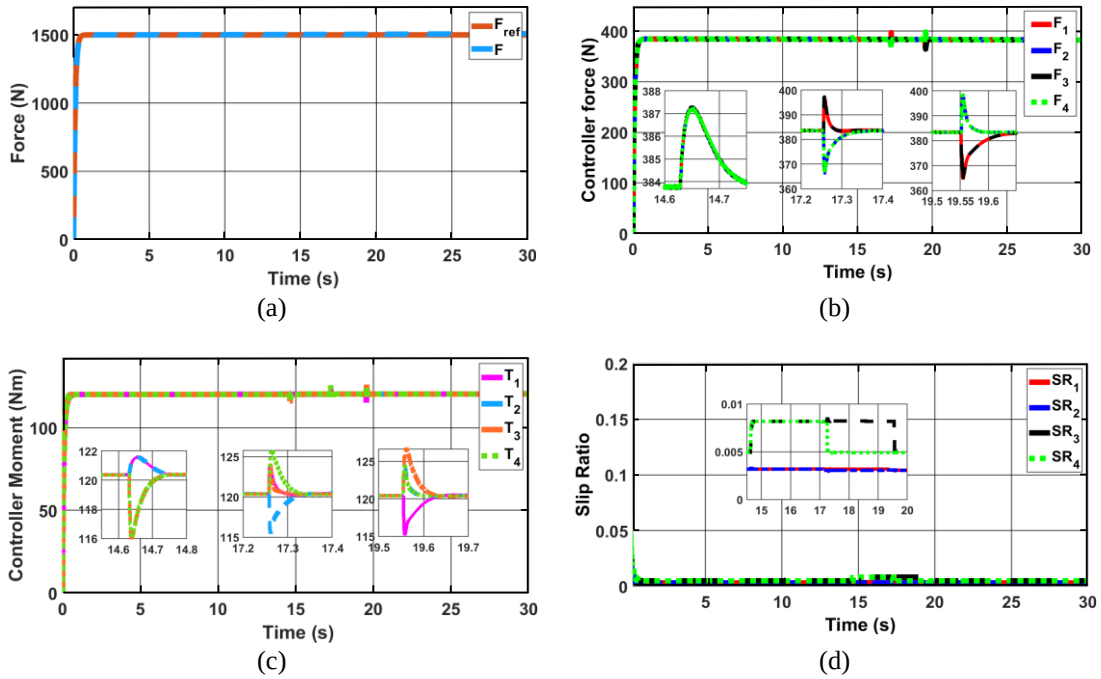

Figure 5. Simulation results: (a) total applied traction force, (b) 4-wheel traction force, (c) 4-wheel moment, and (d) 4-wheel slip

From Figures 6(a) to (d) showing the traction force responses of the traction force observer: Figure 6(a) is the steering force response of the front left wheel; Figure 6(b) is the steering force response of front right wheel; Figure 6(c) is the steering force response of rear left wheel; Figure 6(d) is the steering force

response of rear right wheel. The observed traction forces of all four wheels closely match the feedback traction forces, indicating that the observer's equations can accurately calculate the traction force responses.

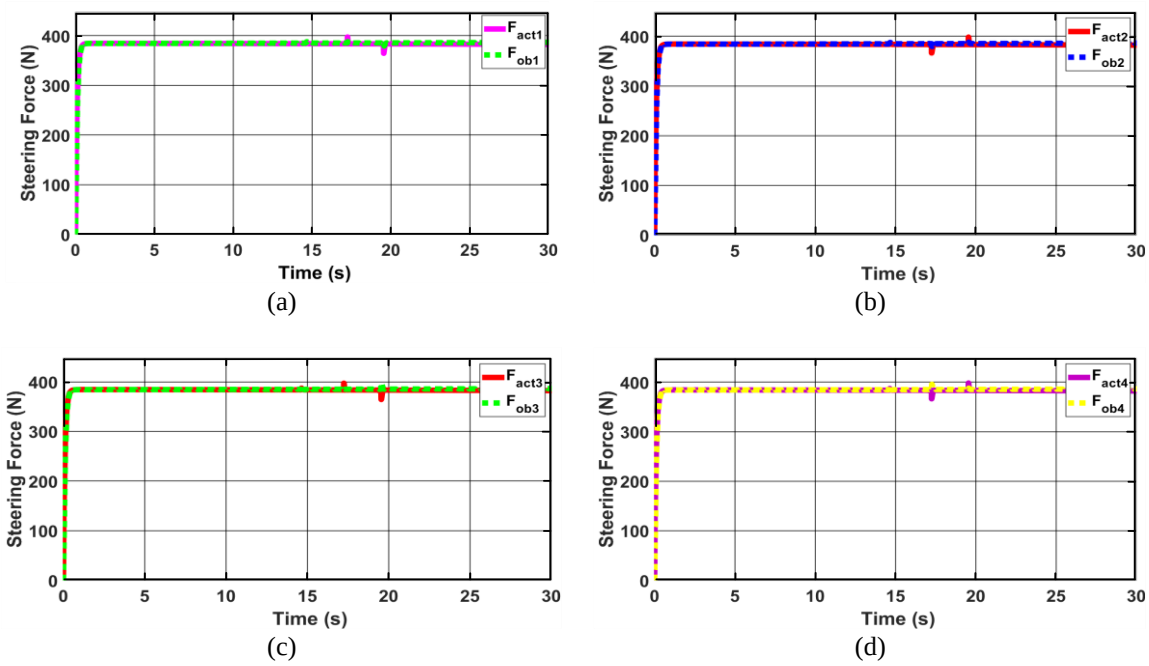

Figure 6. Four-wheel traction response: (a) front left wheel traction response, (b) front right wheel traction response, (c) rear left wheel traction response, and (d) rear right wheel traction response

5. CONCLUSION

This paper successfully presents and validates a method utilizing a traction force observer in conjunction with a speed sliding mode controller to significantly enhance the stability of EVs. The efficacy of this proposed system was comprehensively demonstrated through simulations conducted on a software platform combining MATLAB/Simulink and CarSim. The simulation results conclusively show that this integrated method effectively maintains vehicle stability, minimizes wheel slip, and enhances the overall control system's response even under complex and varying operating conditions. Specifically, the traction force observer proved highly accurate in determining slip by closely matching observed traction forces with feedback traction forces across all four wheels, thereby improving the controller's feedback capability. The sliding mode controller for speed ensured that the system maintained the desired speed and stability throughout the operation, with vehicle and wheel speeds showing only slight and insignificant fluctuations even when encountering slippery road conditions (e.g., snow roads with a friction coefficient of 0.2). The proposed system achieved well-balanced traction force distribution among the wheels, with distributed forces closely following the total applied force of 1500 N, and successfully managed torque adjustments to maintain total traction force alignment with the set value when road conditions changed. Critically, the slip ratio remained approximately zero even when driving on snowy roads, definitively indicating stable vehicle operation without wheel slippage. The achieved results not only open up a promising path for the development of advanced control methods in EVs but also lay a strong foundation for further research and improvement of other control solutions to optimize the performance and operation of EVs in the future.

FUNDING INFORMATION

Our paper is financially supported by the University of Transport and Communications (UTC).

AUTHOR CONTRIBUTIONS STATEMENT

This journal uses the Contributor Roles Taxonomy (CRediT) to recognize individual author contributions, reduce authorship disputes, and facilitate collaboration.

Name of Author	C	M	So	Va	Fo	I	R	D	O	E	Vi	Su	P	Fu
An Thi Hoai Thu Anh	✓	✓	✓	✓	✓	✓		✓	✓	✓			✓	✓
Nguyen Van Hoa			✓		✓	✓			✓					

C : **C**onceptualization
M : **M**ethodology
So : **So**ftware
Va : **Va**lidation
Fo : **Fo**rmal analysis
I : **I**nvestigation
R : **R**esources
D : **D**ata Curation
O : Writing - **O**riginal Draft
E : Writing - Review & **E**diting
Vi : **Vi**sualization
Su : **Su**pervision
P : **P**roject administration
Fu : **Fu**nding acquisition

CONFLICT OF INTEREST STATEMENT

Authors state no conflict of interest.

DATA AVAILABILITY

The data that support the findings of this study are available from the corresponding author, [initial: A.T.H.T.A], upon reasonable request. All simulation data used in this work were generated in MATLAB/Simulink and CarSim environments for research purposes.

REFERENCES

[1] Y. Li, O. P. Adeleke, and X. Xu, "Methods and applications of energy saving control of in-wheel motor drive system in electric vehicles: A comprehensive review," *Journal of Renewable and Sustainable Energy*, vol. 11, no. 6, Nov. 2019, doi: 10.1063/1.5129070.

[2] J. Liu and X. Wang, "Experimental study of the effect of different pulse charging patterns on lithium-ion battery charging," *Journal of Power Sources*, vol. 610, p. 234700, 2024. doi: 10.1016/j.jpowsour.2024.234700.

[3] A. Agrawal *et al.*, "Mathematical Modeling of Driving Forces of an Electric Vehicle for Sustainable Operation," *IEEE Access*, vol. 11, pp. 95278–95294, 2023, doi: 10.1109/ACCESS.2023.3309728.

[4] A. Jo, H. Lee, D. Seo, and K. Yi, "Model-reference adaptive sliding mode control of longitudinal speed for autonomous vehicles," *Proceedings of the Institution of Mechanical Engineers, Part D: Journal of Automobile Engineering*, vol. 237, no. 2-3, pp. 493-515, 2023, doi: 10.1177/09544070221077743.

[5] B. J. Kim and H. Peng, "Optimal vehicle motion control to mitigate secondary crashes after an initial impact," *ASME 2014 Dynamic Systems and Control Conference, DSCC 2014*, vol. 1, 2014, doi: 10.1115/dscc2014-6080.

[6] K. Berntorp, B. Olofsson, K. Lundahl, and L. Nielsen, "Models and methodology for optimal trajectory generation in safety-critical road-vehicle manoeuvres," *Vehicle System Dynamics*, vol. 52, no. 10, pp. 1304–1332, Oct. 2014, doi: 10.1080/00423114.2014.939094.

[7] Z. Liang, J. Zhao, B. Liu, Y. Wang, and Z. Ding, "Velocity-Based Path Following Control for Autonomous Vehicles to Avoid Exceeding Road Friction Limits Using Sliding Mode Method," *IEEE Transactions on Intelligent Transportation Systems*, vol. 23, no. 3, pp. 1947–1958, Mar. 2022, doi: 10.1109/TITS.2020.3030087.

[8] J. Wang, L. Alexander, and R. Rajamani, "Friction estimation on highway vehicles using longitudinal measurements," *Journal of Dynamic Systems, Measurement and Control, Transactions of the ASME*, vol. 126, no. 2, pp. 265–275, Jun. 2004, doi: 10.1115/1.1766028.

[9] K. B. Singh, M. A. Arat, and S. Taheri, "An intelligent tire based tire-road friction estimation technique and adaptive wheel slip controller for antilock brake system," *Journal of Dynamic Systems, Measurement and Control, Transactions of the ASME*, vol. 135, no. 3, May 2013, doi: 10.1115/1.4007704.

[10] N. M. Adam, A. Irawan, and M. A. Ahmad, "Robust super-twisting sliding mode controller for the lateral and longitudinal dynamics of rack steering vehicle," *Bulletin of Electrical Engineering and Informatics*, vol. 11, no. 4, pp. 1882–1891, Aug. 2022, doi: 10.11591/eei.v11i4.3641.

[11] Y. Li, X. Zhang, and H. Sun, "Fault-tolerant control of induction motor with current sensors based on dual-torque model," *Energies*, vol. 16, no. 8, p. 3442, 2023, doi: 10.3390/en16083442.

[12] K. B. Singh, M. A. Arat, and S. Taheri, "Literature review and fundamental approaches for vehicle and tire state estimation," *Vehicle System Dynamics*, vol. 57, no. 11, pp. 1643–1665, Nov. 2019, doi: 10.1080/00423114.2018.1544373.

[13] M. Mazo and P. Tabuada, "Special issue technical notes and correspondence: Decentralized event-triggered control over wireless sensor/actuator networks," *IEEE Transactions on Automatic Control*, vol. 56, no. 10, pp. 2456–2461, Oct. 2011, doi: 10.1109/TAC.2011.2164036.

[14] V. D. Colli, G. Tomassi, and M. Scarano, "Single wheel, longitudinal traction control for electric vehicles," *IEEE Transactions on Power Electronics*, vol. 21, no. 3, pp. 799–808, May 2006, doi: 10.1109/TPEL.2006.872363.

[15] L. Jin and Y. Liu, "Study on adaptive slid mode controller for improving handling stability of motorized electric vehicles," *Mathematical Problems in Engineering*, vol. 2014, no. 1, Jan. 2014, doi: 10.1155/2014/240857.

[16] M. Ringdorfer and M. Horn, "Development of a wheel slip actuator controller for electric vehicles using energy recuperation and hydraulic brake control," in *Proceedings of the IEEE International Conference on Control Applications*, Sep. 2011, pp. 313–318. doi: 10.1109/CCA.2011.6044472.

[17] L. Q. Jin, M. Ling, and W. Yue, "Tire-road friction estimation and traction control strategy for motorized electric vehicle," *PLoS ONE*, vol. 12, no. 6, p. e0179526, Jun. 2017, doi: 10.1371/journal.pone.0179526.

[18] F. Jia, Z. Liu, H. Zhou, and W. Chen, "A novel design of traction control based on a piecewise-linear parameter-varying technique for electric vehicles with in-wheel motors," *IEEE Transactions on Vehicular Technology*, vol. 67, no. 10, pp. 9324–9336, Oct. 2018, doi: 10.1109/TVT.2018.2863035.

[19] H. Hasan, F. A. Samman, M. Anshar, and R. S. Sadjad, "Autonomous vehicle tracking control for a curved trajectory," *Bulletin of Electrical Engineering and Informatics*, vol. 13, no. 3, pp. 1535–1545, Jun. 2024, doi: 10.11591/eei.v13i3.6060.
[20] U. K. and L. Nielsen, "Automotive Control Systems: For Engine, Driveline, and Vehicle," *Measurement Science and Technology*, vol. 11, no. 12, pp. 1828–1828, Dec. 2000, doi: 10.1088/0957-0233/11/12/708.
[21] J. Kong, M. Pfeiffer, G. Schildbach, and F. Borrelli, "Kinematic and dynamic vehicle models for autonomous driving control design," in *IEEE Intelligent Vehicles Symposium, Proceedings*, vol. 2015, pp. 1094–1099, 2015, doi: 10.1109/IVS.2015.7225830.
[22] B. Kunjunni, M. A. B. Zakaria, A. P. P. Majeed, A. F. A. Nasir, M. H. B. Peeie, and U. Z. A. Hamid, "Effect of load distribution on longitudinal and lateral forces acting on each wheel of a compact electric vehicle," *SN Applied Sciences*, vol. 2, no. 2, 2020, doi: 10.1007/s42452-020-1996-9.
[23] Z. Zhang, C.-g. Liu, X. J. Ma, Y. Y. Zhang, and L. M. Chen, "Driving force coordinated control of an 8×8 in-wheel motor drive vehicle with tire-road friction coefficient identification," *Defence Technology*, vol. 18, no. 1, pp. 119–132, Jan. 2022, doi: 10.1016/j.dt.2020.06.006.
[24] E. Esmailzadeh, G. R. Vosspughi, and A. Goodarzi, "Dynamic modeling and analysis of a four motorized wheels electric vehicle," *Vehicle System Dynamics*, vol. 35, no. 3, pp. 163–194, 2001, doi: 10.1076/vesd.35.3.163.2047.
[25] L. Feng, M. Deng, S. Xu, and D. Huang, "Speed Regulation for PMSM Drives Based on a Novel Sliding Mode Controller," *IEEE Access*, vol. 8, pp. 63577–63584, 2020, doi: 10.1109/ACCESS.2020.2983898.
[26] J. Liu and X. Wang, "Advanced Sliding Mode Control for Mechanical Systems," *Advanced Sliding Mode Control for Mechanical Systems*, 2011, doi: 10.1007/978-3-642-20907-9.
[27] P. Latosiński, "Sliding mode control based on the reaching law approach-A brief survey," in *2017 22nd International Conference on Methods and Models in Automation and Robotics, MMAR 2017*, 2017, pp. 519–524, doi: 10.1109/MMAR.2017.8046882.

BIOGRAPHIES OF AUTHORS

An Thi Hoai Thu Anh received her Engineering 1997, and M.Sc. (2002) degrees in Industrial Automation Engineering from Hanoi University of Science and Technology and completed Ph.D. degree in 2020 from the University of Transport and Communications (UTC). Now, she is a lecturer at the Faculty of Electrical and Electronic Engineering at the University of Transport and Communications (UTC). Her interests include power electronic converters, electric motor drives, and energy-saving solutions for industry and transportation. She can be contacted at email: htanh.ktd@utc.edu.vn.

Nguyen Van Hoa is a fourth-year student majoring in Electrical Engineering at the University of Transport and Communications (UTC), Vietnam. His current interests include power electronics and electric drive control, which are applied in the transportation and industry. He can be contacted at email: hoa201503763@lms.utc.edu.vn.